原 著

Analysis of Axial Blood Flow Velocity and Effects of Torsion and Geometric Factors in the Intramyocardial Coronary Arterial Flow by Helical Tube Model : Theoretical Study

Hirohumi Hirayama*, Yuzo Fukuyama*

Abstract

A theoretical investigation was intended to disclose the distributions of the axial blood flow velocity, its spatial rates of changes, the effects of geometric factor and the torsion of intra myocardial coronary arterial system which constitution is characterized by a helical tube model. Mathematical method was based on the modified orthogonal coordinate system. The modified Navier-Stokes equations were solved analytically by power series expansion of the Dean number.

The distribution axial flow velocity skewed laterally. The rate of change of axial velocity W in radial direction on the inner wall surface dW/dr (r=1) increased in the upper hemisphere and decreased in the lower hemisphere. The rate of change in the W at circumferential direction on the inner wall surface dW/d θ (r=1) decreased in the lateral hemisphere and increased in the inner hemisphere. The absolutes of the dW/dr (r=1) and dW/d θ (r=1) increased in larger radius, elevated in the extended state and were larger in 4 times coiling than 2 times coiling.

Key words : Intramyocardial coronary artery, Blood flow velocity, Helical tube, Shear stress.

*Department of Public Health, Asahikawa Medical College, Asahikawa, Japan

Introduction

Many experimental investigations have been accumulated concerning about the blood flow in the coronary artery on the surface of ventricle. The intra myocardial coronary artery, on the other hand, is helically coiled. Thus, it is difficult to measure the blood flow velocity and the shear stress in spatial domain. Certainly a simulation study has reported (1) a blood flow velocity profile, it did not make clear the effects derived in the helical nature of intra myocardial coronary arterial system.

Present investigation was intended to show the distributions of axial flow velocity and its rates of spatial changes in the intra myocardial coronary artery with the influences of torsion and geometric factors based on a mathematical modeling of intramyocardial coronary artery by a helical tube.

Mathematical method

Present theoretical analysis was based on the modified orthogonal coordinate system for a helical tube (2). We set following assumptions for diastolic coronary arterial blood flow within the myocardium : 1) . The flow is steady ; 2) . The radius of artery is constant ; and 3) . The interactions among the blood cells and the arterial wall surface do not exist. Fig 1-a shows the helical tube model of the intra myocardial coronary vessel. The radius of helical tube is a, the pitch of the helix is b and the distance from the central axis of the coordinate to the center of the helical tube is c. Fig 1-b is the modified orthogonal coordinate system of a helical tube. s' is the central axis line of the helical tube, T is the unit tangential vector to s', N is the normal vector and B is the rectangular vector to N. Then

$$dT/ds' = \kappa N \quad (1\text{-a}) \qquad dN/ds' = \tau B - \kappa T \quad (1\text{-b})$$
$$dB/ds' = -\tau N \quad (1\text{-b})$$

where $\kappa = b/(b^2 + c^2)$ is the curvature and $\tau = c/(b^2 + c^2)$ is the torsion. An arbitrary point E on the cross section is expressed by the positional vector R in the Cartesian coordinate as a function of (s', r', θ)

$$R = Ro(s') - r'\cos(\theta + \phi)N(s') + r'\sin(\theta + \phi)B(s').$$

where Ro (s') is the central positional vector in the helical tube and r' is the distance from the point E to the central point. We introduce following new vectors for the convenience

Fig 1-a

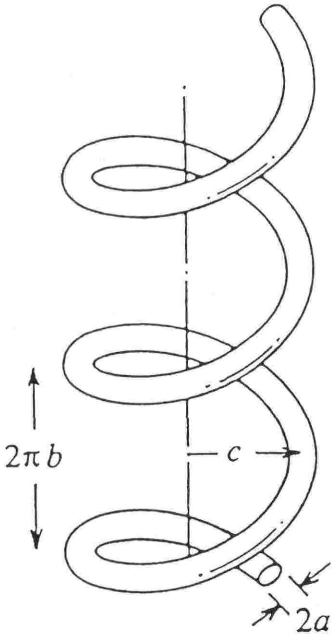

Fig 1-b

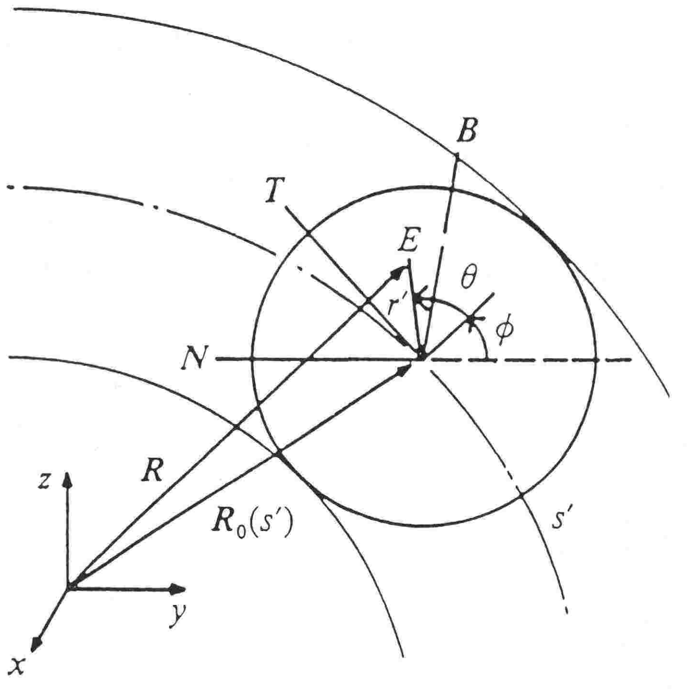

Fig 1. Modeling of intramyocardial coronary arterial system by a helical tube.

Fig 1-a The schematic illustration of intramyocardial coronary artery by a helical tube. a is the radius of artery. b is the pitch of helical tube. c is the distance between the center of coordinate system, which is normal to the tangential surface plane of ventricle, and the center of cross sectional plane of helical tube.

Fig 1-b The circle in the figure is one cross sectional plane in the helical tube. s' is the center line of a helical tube. θ is the circumferential angle of the cross sectional plane with 0 at the outer wall and π at the inner wall. ϕ expresses the initial rotation angle of the helical flow and can be ignored in a fully developed flow. E is an arbitrary point of the cross section defined by a Cartesian position vector R.

$$ar = \sin(\theta+\phi)B - \cos(\theta+\phi)N \qquad (2\text{-a})$$
$$a\theta = \cos(\theta+\phi)B + \sin(\theta+\phi)N \qquad (2\text{-b})$$

where angle ϕ is supplemental circumferential angle defined as

$$\phi(s') = \int_{S'o}^{S'} \tau(s)\,dS'o$$

Then the metric of this system is

$$dR = ds'[1+\kappa r'\cos(\theta+\phi)]T + dr'\,ar + r'\,d\theta\,a\theta$$

With the aid of the orthogonal metric, the Navier Stoke equations for steady flow in the coordinates s', r', θ are

$$w\frac{\partial W}{\partial s'} + \frac{\partial U}{\partial r'} + \frac{U}{r'} + \frac{1}{r'}\frac{\partial V}{\partial \theta} + \kappa w[\cos(\theta+\phi)U - \sin(\theta+\phi)V] = 0 \qquad \cdots\cdots(3)$$

$$DW + \kappa wW[\cos(\theta+\phi)U - \sin(\theta+\phi)V] = -w\frac{\partial p}{\partial s'} + \nu\left[\left(\frac{1}{r'} + \frac{\partial}{\partial r'}\right)\times\left(\frac{\partial W}{\partial r'} + \kappa w\cos(\theta+\phi)W - w\frac{\partial U}{\partial s'}\right) + \frac{1}{r'}\frac{\partial}{\partial \theta}\left(\frac{1}{r'}\frac{\partial W}{\partial \theta} - \kappa w\sin(\theta+\phi)W - w\frac{\partial V}{\partial s'}\right)\right] \qquad \cdots\cdots(4)$$

$$DU - \frac{V^2}{r'} - \kappa w\cos(\theta+\phi)W^2 = -\frac{\partial p}{\partial r'} + \nu\left[\left(\frac{1}{r'}\frac{\partial}{\partial \theta} - \kappa w\sin(\theta+\phi)\right)\times\left(\frac{1}{r'}\frac{\partial U}{\partial \theta} - \frac{\partial V}{\partial r'} - \frac{V}{r'}\right) - w\frac{\partial}{\partial s'}\left(\frac{\partial W}{\partial r'} + \kappa w\cos(\theta+\phi)W - w\frac{\partial U}{\partial s'}\right)\right] \qquad \cdots\cdots(5)$$

$$DV + \frac{UV}{r'} + \kappa w\sin(\theta+\phi)W^2 = -\frac{1}{r'}\frac{\partial p}{\partial \theta} + \nu\left[w\frac{\partial}{\partial s'}\left(w\frac{\partial V}{\partial s'} + \kappa w\sin(\theta+\phi)W - \frac{1}{r'}\frac{\partial W}{\partial \theta}\right) - \left(\frac{\partial}{\partial r'} + \kappa w\cos(\theta+\phi)\right)\left(\frac{1}{r'}\frac{\partial U}{\partial \theta} - \frac{\partial V}{\partial r'} - \frac{V}{r'}\right)\right] \qquad \cdots\cdots(6)$$

where U, V and W are the velocity components in the ar, a θ and T directions respectively. P is the input diastolic pressure, ν is the kinematic viscosity. $w = 1/(1+\kappa r'\cos(\theta+\phi))$ and D is a differential operator defined as

$$D = wW\frac{\partial}{\partial s'} + U\frac{\partial}{\partial r'} + \frac{V}{r'}\frac{\partial}{\partial \theta'}$$

Setting new variables as following for the simplicity of mathematical treatment,

$$r = r'/a, \qquad \varepsilon = a\kappa, \qquad \lambda = a\tau$$
$$u = aU/\nu,\ v = aV/\nu$$
$$w = (2\kappa a^3)^{1/2}W/\nu \qquad D = G\,a^2(2\kappa a^3/\nu^2)^{1/2}/\mu \qquad \cdots\cdots(7)$$

where G is pressure gradient of input pressure, μ is the viscosity (0.03P). The boundary conditions are

$$u = v = w = 0 \quad \text{at} \quad r = 1.0 \qquad \cdots\cdots(8)$$

The pressure terms in (5) and (6) are removed by cross differentiation. Then

$$\frac{\partial v}{\partial \alpha} + \frac{\partial}{\partial r}(ru) + \beta^{\frac{1}{2}}r\frac{\partial w}{\partial \alpha} = 0 \qquad \cdots\cdots(9)$$

$$\nabla^2 w - u\frac{\partial w}{\partial r} - \frac{v}{r}\frac{\partial w}{\partial \alpha} = -D + \beta^{\frac{1}{2}}w\frac{\partial w}{\partial \alpha} \qquad \cdots\cdots(10)$$

$$\nabla^2\Omega - \frac{1}{r}u\Omega - \frac{\partial}{\partial r}(u\Omega) - \frac{1}{r}\frac{\partial}{\partial \alpha}(v\Omega) = w\left(\sin\alpha\frac{\partial w}{\partial r} + \frac{1}{r}\cos\alpha\frac{\partial w}{\partial \alpha}\right) + \beta^{\frac{1}{2}}\left(w\frac{\partial \Omega}{\partial \alpha} - \frac{1}{r}\frac{\partial w}{\partial \alpha}\frac{\partial u}{\partial \alpha} + \frac{\partial w}{\partial r}\frac{\partial v}{\partial \alpha}\right) \qquad \cdots\cdots(11)$$

where Ω is the dimensionless vorticity for the secondary flow. ∇^2 is the differential operator defined as

$$\Omega=\frac{\partial v}{\partial r}+\frac{v}{r}-\frac{1}{r}\frac{\partial u}{\partial(\theta+\phi)}$$

$$\nabla^2=\partial^2/\partial r^2+1/r\ \partial/\partial r+1/r^2\ \partial^2/\partial\alpha^2$$

and

$$\alpha=\theta+\phi,\ \beta^{1/2}=\lambda/(2\varepsilon)^{1/2}.$$

Here we set

$$\bar{u}=u,\ \bar{v}=v,\ \bar{w}=Dw/4\qquad \bar{\Omega}=\Omega\quad D/4=K^{1/2}$$

where the quantities with bars denote Dean's variables and K is the original Dean number defined by Dean (3). By these conversions, the differential equations (9), (10) and (11) are reduced to

$$\frac{\partial v}{\partial\alpha}+\frac{\partial}{\partial r}(ru)=-\beta^{\frac{1}{2}}K^{\frac{1}{2}}r\frac{\partial\bar{w}}{\partial\alpha},\qquad\cdots\cdots(12)$$

$$\nabla^2\bar{w}-\left(u\frac{\partial\bar{w}}{\partial r}+\frac{v}{r}\frac{\partial\bar{w}}{\partial a}\right)$$
$$=-4+\beta^{\frac{1}{2}}K^{\frac{1}{2}}\bar{w}\frac{\partial\bar{w}}{\partial\alpha}\qquad\cdots\cdots(13)$$

$$\nabla^2\Omega-\left(u\frac{\partial\Omega}{\partial r}+\frac{u}{r}\frac{\partial\Omega}{\partial\alpha}\right)$$
$$=K\bar{w}\left(\sin\alpha\frac{\partial\bar{w}}{\partial r}+\frac{\cos\alpha}{r}\frac{\partial\bar{w}}{\partial\alpha}\right)$$
$$+\beta^{\frac{1}{2}}K^{\frac{1}{2}}\left(\bar{w}\frac{\partial\Omega}{\partial\alpha}-\Omega\frac{\partial\bar{w}}{\partial\alpha}\right)$$
$$-\beta^{\frac{1}{2}}K^{\frac{1}{2}}\left(\frac{1}{r}\frac{\partial\bar{w}}{\partial\alpha}\frac{\partial u}{\partial\alpha}-\frac{\partial\bar{w}}{\partial r}\frac{\partial v}{\partial\alpha}\right)\qquad\cdots\cdots(14)$$

By introducing a modified stream function ϕ to replace the continuity equation (12),

$$u=\frac{1}{r}\frac{\partial\Psi}{\partial\alpha}-\beta^{\frac{1}{2}}K^{\frac{1}{2}}\frac{1}{r}\int_0^r r\frac{\partial\bar{w}}{\partial\alpha}dr$$
$$u=-\frac{\partial\Psi}{\partial r}\qquad\cdots\cdots(15)$$

Present system equations are converted to equation (16) and (17).

$$\nabla^2\bar{w}+4=\frac{1}{r}\left(\frac{\partial\Psi}{\partial x}\frac{\partial\bar{w}}{\partial r}-\frac{\partial\Psi}{\partial r}\frac{\partial\bar{w}}{\partial\alpha}\right)+\beta^{\frac{1}{2}}K^{\frac{1}{2}}$$
$$\left(\bar{w}\frac{\partial\bar{w}}{\partial\alpha}-\frac{1}{r}\frac{\partial\bar{w}}{\partial r}\int_0^r r\frac{\partial\bar{w}}{\partial\alpha}dr\right)\qquad\cdots\cdots(16)$$

$$\nabla^4\Psi=\frac{1}{r}\left(\frac{\partial\Psi}{\partial\alpha}\frac{\partial}{\partial r}-\frac{\partial\Psi}{\partial r}\frac{\partial}{\partial\alpha}\right)\nabla^2\Psi$$
$$+\beta^{\frac{1}{2}}K^{\frac{1}{2}}\left[\frac{1}{r^4}\int_0^r r\left(4\frac{\partial^2\bar{w}}{\partial\alpha^2}+\frac{\partial^4\bar{w}}{\partial\alpha^4}\right)dr\right.$$
$$+\frac{2}{r^4}\frac{\partial\Psi}{\partial\alpha}\int_0^r r\frac{\partial^2\bar{w}}{\partial\alpha^2}dr+\frac{1}{r^3}\frac{\partial\Psi}{\partial r}$$
$$\left.\int_0^r r\frac{\partial^3\bar{w}}{\partial\alpha^3}dr-\frac{1}{r}\frac{\partial}{\partial r}\nabla^2\psi\int_0^r r\frac{\partial\bar{w}}{\partial\alpha}dr\right]$$
$$+\beta^{\frac{1}{2}}K^{\frac{1}{2}}\left[\frac{1}{r}\frac{\partial^3\bar{w}}{\partial r\partial\alpha^2}-\frac{1}{r^2}\left(2+\frac{\partial\psi}{\partial\alpha}\right)\frac{\partial^2\bar{w}}{\partial\alpha^2}\right.$$
$$-\left(\frac{\partial\bar{w}}{\partial\alpha}-\bar{w}\frac{\partial}{\partial\alpha}\right)\nabla^2\Psi+\frac{1}{r^2}\frac{\partial\bar{w}}{\partial\alpha}\frac{\partial^2\psi}{\partial\alpha^2}$$
$$\left.+\frac{\partial\bar{w}}{\partial r}\frac{\partial^2\psi}{\partial r\partial\alpha}\right]+K\left[-\bar{w}\left(\sin\alpha\frac{\partial\bar{w}}{\partial r}\right.\right.$$
$$\left.+\frac{\cos\alpha}{r}\frac{\partial\bar{w}}{\partial\alpha}\right)+\frac{\beta}{r^2}\int_0^r r\frac{\partial\bar{w}}{\partial\alpha}dr\left(\frac{\partial^2\bar{w}}{\partial\alpha^2}\right.$$
$$\left.-\frac{2}{r^2}\int_0^r r\frac{\partial^2\bar{w}}{\partial\alpha^2}dr\right)$$
$$\left.-\frac{\beta}{r^2}\bar{w}\int_0^r r\frac{\partial^3\bar{w}}{\partial\alpha^3}dr\right]\qquad\cdots\cdots(17)$$

The boundary conditions for these modified differential equations are

$$\bar{w}=0,\ \frac{\partial\Psi}{\partial r}=0,\ \Psi=\beta^{\frac{1}{2}}K^{\frac{1}{2}}\int_0^\alpha\int_0^1 r\frac{\partial\bar{w}}{\partial\alpha}dr d\alpha$$
at $r=1$, $\qquad\cdots\cdots(18)$

In a fully developed flow, ϕ is arbitrary and can be neglected. This system can be solved by expanding the solutions in the powers of small Dean number K as

$$w=w_0+Kw_1+K^{3/2}w_2+K^2w_3+K^{5/2}w_4+****$$
$$\psi=\psi_0+K\psi_1+K^{3/2}\psi_2+K^2\psi_3+K^{5/2}\psi_4+****$$

Fluid dynamical significance of the parameters.

The Dean number K is equal to the ratio of the square root of the product of the inertial force and the centrifugal force to the viscous force. The Dean number is a measure of the magnitude of the secondary flow produced by the centrifugal force that originated from the curvature effect and its interaction to the viscous force. The curvature rate δ is a measure of the effect of geometry and the extent to which the centrifugal force varies on the cross section. The 0th order solution is identical with the Poiseulli flow ($wo = 1 - r^2$), while wn and ψ n (n> 1) can be expressed by serial expansions of the r such that

$$w1 = f_1(r)\cos\alpha,\ w2 = f_2(r)\cos\alpha + f_3(r)\sin\alpha,$$
$$w3 = f_4(r) + f_5(r)\cos 2\alpha + f_6(r)\cos\alpha + f_7(r)\sin\alpha,\ \psi 1 = g_1(r)\sin\alpha\quad \psi 2 = g_2(r)\cos\alpha$$
$$\psi 3 = g_3(r)\sin 2\alpha + g_4(r)\cos\alpha + g_5(r)\sin\alpha$$

We have analyzed the effects of changes in the radius, the geometric factor $\delta = a/c$ and the torsion on the intra myocardial coronary arterial system by setting

1) the dilatated state (a = 0.1cm : KW1, KW2, KW3, KW4 in the table 1) and the constricted state (a = 0.04cm: KW5, KW6, KW7, KW8 in the table 1) of the helical tube,

2) the extended state ($c = \pi b$: KW1, KW3, KW5, KW7) and the compressed state ($c=4\pi b$: KW2, KW4, KW6, KW8) of the helical tube.

3) The effects of torsion were examined by alternating the number of helical rotations by 2 times (KW1, KW2, KW5, KW6) and 4 times (KW3, KW4, KW7, KW8).

Each case was expressed by the KWn. The values of the parameters a, b, c, δ (the curvature ratio = a/c), ε, τ, κ, λ, $\beta^{1/2}$ and K were shown in Table 1. The thickness of ventricular muscle was set to be 1.5cm. The anatomical relations between the pitch b and the distance from the center of the helical tube to the axis of coordinate, c, have yet be known. Thus, we have assumed that the intra myocardial coronary artery is created in a compact cubic form within a given volume of ventricular muscle. Thus the relation $2\pi b = 2C$ was assumed. Because by the n times rotations, the intra myocardial vessel reaches to the endocardium from the epicardial surface of the ventricle, $2\pi b n = 1.5$cm. Thus b, c and n were not independent but are inter related parameters. For the simplicity we set driving pressure gradient G = 1.0.

Results (Fig 2)

The axial flow velocity W was positive in the entire cross sectional plane of the helical tube. The maximum of W was attained at $\theta = \pi/4$ and $\theta = 7$

Table 1 System Parameters

	a (cm)	b (cm)	c (cm)	δ	n	
KW 1	0.1	0.1194	0.375	1/3.75	2	$c=\pi b$
KW 2	0.1	0.1194	1.499	1/14.9	2	$c=4\pi b$
KW 3	0.1	0.0597	0.1875	1/1.875	4	$c=\pi b$
KW 4	0.1	0.0597	0.75	1/7.5	4	$c=4\pi b$
KW 5	0.04	0.1194	0.375	1/9.375	2	$c=\pi b$
KW 6	0.04	0.1194	1.4996	1/37.49	2	$c=4\pi b$
KW 7	0.04	0.0597	0.1875	1/4.6875	4	$c=\pi b$
KW 8	0.04	0.0597	0.75	1/18.75	4	$c=4\pi b$
	κ	τ	ε	λ	K	$\beta^{1/2}$
KW 1	2.4212	0.7709	0.242	0.07709	0.2037	0.1105
KW 2	0.6626	0.0527	0.06626	0.00527	0.005575	0.0145
KW 3	4.8424	1.5418	0.48424	0.154	0.0407	0.1566
KW 4	1.3249	0.10546	0.1324	0.010546	0.01114	0.0205
KW 5	2.4212	0.7709	0.0968	0.03083	0.0000337	0.0701
KW 6	0.6626	0.05276	0.026505	0.00211	0.00000913	0.00916
KW 7	4.842	1.5418	0.19369	0.0616	0.00006675	0.0991
KW 8	1.3249	0.1054	0.05299	0.004218	0.00001826	0.01295

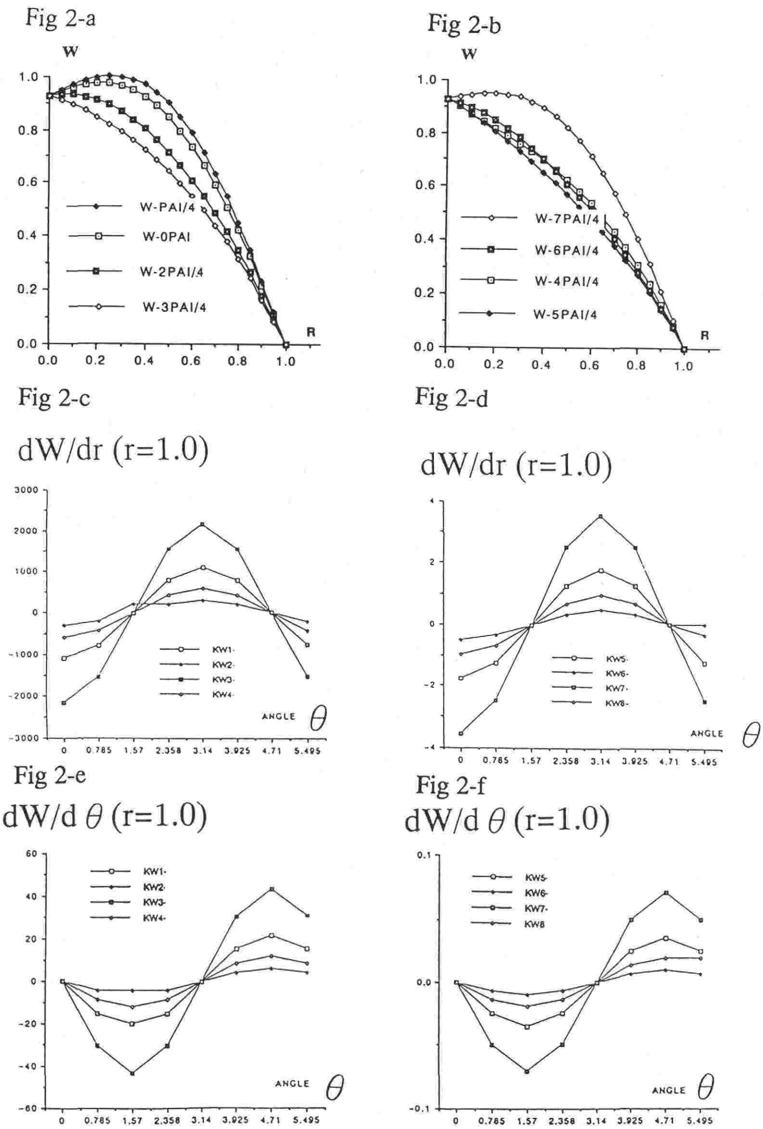

Fig 2. Distribution of the axial blood flow velocity (cm/s) in a cross sectional plane and the rates of spatial changes in axial blood flow velocity dW (cm/s) /dr, dW (cm/s) /d θ on the wall surface in a cross sectional plane. (all the values were expressed by magnified of 10^6)

Fig 2-a shows the blood flow velocity in axial direction W (ordinate) with parametric changes in circumferential angle θ with $\pi/4$ step increase. The Fig 2-a indicates the axial flow velocity W in $0<\theta<3\pi/4$ (upper hemisphere) and the Fig 2-b expresses the axial velocity in $\pi<\theta<7\pi/4$ (lower hemisphere).

Fig 2-c shows the circumferential distribution of rate of change in axial flow velocity W in radial direction dW/dr (r=1.0). The abscissa is the circumferential angle measure from the outer wall ($\theta=0$) to the top of the cross section ($\theta=1.57$), the inner most wall ($\theta=3.14$), the bottom of the cross section ($\theta=3.14$) and again the lateral wall ($\theta=6.28$). The upper parts of the Fig 2-c are those for larger radius (a=0.1 cm) while the lower part of the Fig 2-d are those for smaller radius (a=0.04 cm) respectively. The dW/dr (r=1.0) indicated by KWn are calculated by the combination of the parameters given in Table 1. Fig 2-e and Fig 2-e and Fig 2-f show the rate of change in W in circumferential direction θ dW/d θ (r=1.0).

$\pi/4$ with r =0.24. The distribution of the axial velocity skewed laterally due to the centrifugal force.

The rate of change of the W in the radial direction on the wall surface dW/dr (r = 1.0) (Fig 2-a) was negative in the lateral hemisphere ($0 < \theta < \pi/2$ and $3\pi/2 < \theta < 2\pi$) while it was positive in the inner hemisphere ($\pi/2 < \theta < 3\pi/2$). The dW/dr (r = 1.0) increased for $0 < \theta < \pi$ and turned to be positive value at the top (θ = 1.57: $\pi/2$) of the cross sectional plane. In the lower hemisphere, The dW/dr (r = 1.0) decreased for $\pi < \theta < 2\pi$ and turned to be negative value at the bottom of the cross section (θ = 4.71: $3\pi/2$).

The change of the W along the circumferential direction on the inner wall surface dW/d θ (r = 1.0) (Fig 3-b) was negative in the upper hemisphere ($0 < \theta < \pi$), while it was positive in the lower hemisphere. In the upper part of the lateral hemisphere ($0 < \theta < \pi/2$), the dW/d θ (r = 1.0) decreased. The most potent deceleration occurred at the top of the cross sectional plane ($\theta = \pi/2$). In the inner hemisphere, the dW/d θ (r = 1.0) increased for $\pi/2 < \theta < 3\pi/2$ which turned to be positive value at $\theta = \pi$.

The absolutes of the dW/dr (r = 1) and dW/d θ (r = 1) increased in a larger radius (a = 0.1cm) than in a smaller radius (a = 0.04cm) (KW1 > KW5, KW2 > KW6, KW3 > KW7 and KW4 > KW8). They increased in the extended state than in the compressed state (KW1 > KW2, KW3 > KW4. KW5 > KW6 and KW7 > KW8). They marked larger values in large number of helical coiling (n = 4) than in the small number (n = 2) (KW3 > KW1, KW4 > KW2, KW7 > KW5 and KW8 > KW6).

Discussion

Present theoretical study analyzed the distribution patterns of the axial blood flow velocity in the intramyocardial coronary artery and its rates of spatial changes. We have shown constitutional properties of intramyocardial artery consisting helical rotation by the effects of geometric factor and torsion of helically coiled tube.

For the simplicity of theoretical treatment, the organization of the helical tube was assumed to be a cubic one. In actual coronary system, however, many other factors includig bifurcation must modify the numbr of helix. In such situation, present theory has to be modified to be a more complicated one. In the present study, the wall of the intra myocardial artery was assumed to be rigid although in actual system, the wall properties are determined by the interaction between the elastic factor of the intra myocadium and the tension of the wall. To incorporate these constitutional factors makes the problem too complicated to solve. More over, the physical analysis of a curved elastic tube has been started only recently and we can find any sufficient comparable theoretical study. Thus these wall properties should be taken into consideration in our future work.

Present results showed that at a given number of helical coiling, the rates of spatial changes in the axial flow velocity on the inner wall surface, dW/dr (r = 1.0), dW/d θ (r = 1.0) were larger in the extended state (larger curvature ratio δ) represented by the KW1, KW3, KW5 and KW7 than in the compressed state KW2, KW4, KW6, KW8. According to the experimental reports in a curved pipe, the mean vorticity (4) increased in a larger δ (= 1/4.66) than in a smaller δ (= 1/8.00). The circumferential wall shear stress (5) was augmented in a larger δ (= 1/7) than in a smaller δ (= 1/20). The wall shear stress (6) was enhanced in a larger δ (= 1/3) than in a smaller δ (= 1/7). Thus present ifluences due to change in the geometric factor (δ) were consistent to the experimental data and the geometric factor plays important roles even in a helical tube at a small Dean number.

The effects of the torsion was quantified by the rotation number n of the helical tube of the intramyocardial coronary arterial system. The rates of spatial change in the axial flow velocity on the inner wall surface increased more by the 4 times helical rotations than by the 2 times coiling (n = 2). More over, large values of $\beta^{1/2}$ (the rate of curvature to torsion) resulted in larger values of the rates of spatial change in the flow velocity (KW3, KW4, KW7, KW8) than smaller $\beta^{1/2}$ (KW1, KW2, KW5, KW6). Thus present data showed that even under small Dean number, the secondary flow is influenced by the torsion. Soh (5), by numerical calculation showed that the circumferential wall shear is enhanced by a larger Dean number than by a smaller Dean number. Bovendeerd (7) reported that the mean vorticity is stronger for a larger Dean number than for a smaller one. Those experimental data are consistent to our data. Therefore at least in the qualitative aspects, our results relevant to the effects of the torsion were consistent to those experimental and theoretical results.

There has been little number of paper that referred to the spatial distribution in shear stress at small Dean number. For fully developed flow (8) in a circular tube at Dean number = 0.7559, the axial shear stress marked higher value at the inner wall than at the outer wall. This result is consistent to the distribution of the dW/dr (r = 1.0) in the present study.

Conclusion

The rates of spatial distribution changes in the radial and the circumferential directions of the axial blood flow velocity in helical model of the intramyocardial artery with the maximum Dean number below 1.0 showed characteristic patterns. They increased with the radius, in the extended state of the helical tube and with the number of helical coiling. Present results are available to speculate the distribution of the shear stress by the axial blood flow in the intramyocardial coronary artery and analyze the disturbance of coronary blood flow in the ischemic heart disease.

References

1) Chang L-J and Tarbell JM. : A numerical study of flow in curved tubes simulating coronary arteries. J Biomechanics 21 : 927-937, 1988
2) Kao, H. : Torsion effect on fully developed flow in a helical pipe. J Fluid Mech 184 : 335-356, 1987
3) Dean WR : The stream line motion of fluid in a curved pipe. Phil Mag J Science 5 : 673-695, 1928
4) Olson E., Snyder B. J : The upstream scale of flow development in curved in curved circular pipes. J Fluid Mech 150 : 139-158, 1985
5) Soh Y. Berger S.A.: Laminar entrance flow in a curved pipe. J Fluid Mech 148 : 109-135, 1984
6) Suzuki J and Tanishita K : Wall shear stress profile of the entrance flow in a strongly curved tube. J J Mech Eng 58 : 1098-1103, 1992
7) Bovendeerd P.H.M. Steenhoven A.A. : Steady entry flow in a curved pipe. J Fluid Mech 177 : 233-246, 1987
8) Hamakiotes CC, Berger SA. : Fully developed pulsatile flow in a curved pipe. J Fluid Mech 195 : 23-22, 1988

(Circ Cont 17 : 535～542, 1996)